

# Improving Robustness and Modeling Generality for Power Flow Analysis

Marko Jereminov\*, David M. Bromberg\*, Xin Li, Gabriela Hug, Larry Pileggi  
Dept. of Electrical and Computer Engineering  
Carnegie Mellon University  
Pittsburgh, PA

**Abstract**— In this paper we present an equivalent circuit model for power system networks that facilitates robust and efficient AC power flow simulation and enables the incorporation of more generalized bus and line models. The circuit equations are formulated in terms of voltages and currents in rectangular coordinates using a graph theoretic algorithm that provides for optimal numerical conditioning. A current-source based generator model is introduced that provides for more robust and efficient convergence as compared to our original approach. We show that the proposed framework supports nonlinear models with insensitivity to the initial guess and converges in few iterations. We illustrate the capabilities of generalized modeling by deriving a model for a grid-connected solar panel system that includes AC, DC and semiconductor components.

**Index Terms**—Power flow, power grid, smart grid, simulation

## I. INTRODUCTION

The transmission and distribution of AC power is typically simulated via power flow analysis. Nonlinear balance equations of real and reactive power are solved to calculate the voltage magnitudes and phases at all load buses, as well as the reactive power and voltage phase of all generators [1]. Of course the true state variables of the physical power grid are voltage and current, since it is an electrical circuit. We have shown that writing the system equations for power balance in terms of voltage magnitude and angles can limit the model complexity and robustness relative to what is achievable when the grid model is described in terms of its true state variables [2].

In this paper we extend the circuit simulation-based approach for AC power flow in [2] that is based on an equivalent circuit formulation of current and voltage variables. Most importantly, we propose a modified generator model that facilitates robust convergence and enables more generalized nonlinear load models. The proposed approach supports any nonlinear function of current and voltage in the same way that a traditional circuit simulator (e.g., SPICE [3]) handles nonlinearities for elements such as diodes and transistors. We describe the proposed formulation and algorithms and illustrate how the choice of state variables can improve robustness and facilitate incorporation of more complex, physical-based models using a grid-connected solar panel system example. Simulations performed on IEEE and Polish system benchmarks [4] demonstrate convergence superior to traditional power flow.

## II. POWER FLOW USING SPLIT CIRCUIT MODEL

We briefly overview our equivalent circuit model based approach for AC power flow analysis [2]. The input to a power flow program is a network of buses linked by transmission lines and transformers. Each of these components is translated to an equivalent circuit based on the underlying relations between voltage and current. The circuit models, which may consist of controlled and independent voltage sources, current sources, and impedances, are all functions of complex variables. Some of the circuit elements are nonlinear, which necessitates the use of a nonlinear solution method. The Newton-Raphson (N-R) method is a preferred algorithm due to its quadratic rate of convergence, but it requires taking a derivative of the nonlinear equations, which is not possible for complex-valued non-analytic functions. To overcome this constraint, we split the equivalent circuit into a real sub-circuit and an imaginary sub-circuit, where the former contains all real-valued voltages and currents and the latter contains all imaginary-valued voltages and currents. The resulting models and functions are differentiable, so that N-R can be applied.

As an example of split circuit modeling, consider a transmission line represented by the pi-model in Figure 1(a). By writing Ohm's law in rectangular coordinates we obtain an expression for current in terms of voltage and admittance:

$$\hat{I} = I_R + jI_I = \hat{Y}\hat{V} = (Y_R + jY_I)(V_R + jV_I) \\ = (Y_R V_R - Y_I V_I) + j(Y_I V_R + Y_R V_I) \quad (1)$$

To split the transmission line into real and imaginary circuits, we find the admittances of the “shunt” portions and the “branch” portion connecting the two shunts of the pi-model. The admittance of the shunt elements is purely imaginary ( $Y_{shunt} = jB/2$ ), but the branch connecting them has both real and imaginary terms ( $Y_{branch} = 1/(R + jX) = R/(R^2 + X^2) - jX/(R^2 + X^2)$ ). Substituting into (1) and extracting the real parts yields:

$$I_{R,branch} = \frac{R}{R^2 + X^2} V_{R,branch} + \frac{X}{R^2 + X^2} V_{I,branch} \quad (2)$$

$$I_{R,shunt} = -\frac{B}{2} V_{I,shunt} \quad (3)$$

The first term in equation (2) represents a conductance, because the real current is proportional to the real voltage; the second term of equation (2), however, represents a voltage-controlled current source, because the real-valued current is proportional to the imaginary voltage. Similar circuit components can be derived for the imaginary parts, leading to the equivalent circuit in Figure 1(b). This procedure of finding relations between current and voltage in rectangular coordinates and splitting the real and imaginary parts is repeated for all buses and lines in the system; see [2] for a full derivation. An example of a nonlinear generator model is given in the following sub-section.

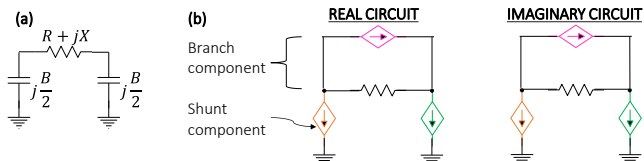


**Figure 1 – (a) Pi-model of transmission line; (b) Split circuit model, with color-coded controlled sources to indicate coupling.**

Once an equivalent circuit model is obtained, the circuit is solved for its voltages and currents. Although Modified Nodal Analysis can be used, in this work, Tree-Link Analysis (TLA) [5]-[6] is employed to formulate the equations [2]. TLA is a graph theoretic approach that offers superior robustness compared to nodal analysis. A “tree” is formed by selecting elements to touch all circuit nodes and form no loops, and we solve for the voltages across these elements; all other elements comprise the “links,” and we solve for their currents. The TLA system of circuit equations is given by (4), where  $v_t$  is a vector of tree branch voltages and  $i_l$  is a vector of link currents.  $R$  is a matrix of resistances used to calculate the voltage across a tree branch from the current flowing through the branch.  $V_t$  is a vector of independent voltage sources that appear on tree branches.  $\alpha$  is a matrix where the only non-zero entries represent dependent voltage sources in the tree that are controlled by link voltages.  $G$  is a matrix of conductances,  $I_l$  a vector of independent current sources, and  $\beta$  a matrix of tree branch current-controlled current sources that appear in the co-tree.  $F$  is a matrix where each row is a fundamental cutset relating a single branch to all other links.

$$\begin{bmatrix} 1 + \alpha F^T & RF \\ -GF^T & 1 + \beta F \end{bmatrix} \begin{bmatrix} v_t \\ i_l \end{bmatrix} = \begin{bmatrix} V_t \\ I_l \end{bmatrix} \quad (4)$$

Components are selected for the tree or links based on their type and the more “natural” variable to solve for; for example, it is clearly simplest to solve for the voltage of an independent voltage source and for the current of an independent current source, and so the former is selected for the tree and the latter for the links. Very small impedances have correspondingly small voltage drops but large currents, and so solving for the voltage by placing these impedances in the tree makes for a better-conditioned system. Likewise, large impedances are best treated in terms of their (small) currents, and so these are selected for the links. This priority ordering can lead to optimally-conditioned matrices for more robust computation. TLA is also capable of handling perfect switches, which is

important for contingency analyses built on top of steady state power flow.

As the equations for voltage and current are nonlinear, we apply the Newton-Raphson algorithm to iteratively compute the solution. On each iteration, model calls are made to update the values of all the nonlinear circuit elements (i.e., those that comprise the generators and loads) according to their respective equations. The linearized TLA system of equations (4) is then updated and solved for new tree branch voltage and link current values.

### III. CURRENT SOURCE-BASED GENERATOR MODEL

In [2], the split circuit model of a generator was derived in terms of voltage. We began by writing the equations for real power ( $P_G$ ) and voltage magnitude ( $|V_G|$ ), which are the known quantities for this bus, in terms of the real and imaginary voltages ( $V_{RG}, V_{IG}$ ) and currents ( $I_{RG}, I_{IG}$ ):

$$P_G = V_{RG}I_{RG} + V_{IG}I_{IG} \quad (5)$$

$$|V_G|^2 = V_{RG}^2 + V_{IG}^2 \quad (6)$$

Solving for the voltages yields the following expressions:

$$V_{RG} = \frac{P_G I_{RG} \pm I_{IG} \sqrt{V_G^2 (I_{RG}^2 + I_{IG}^2) - P_G^2}}{I_{RG}^2 + I_{IG}^2} \quad (7)$$

$$V_{IG} = \frac{P_G I_{IG} \pm I_{RG} \sqrt{V_G^2 (I_{RG}^2 + I_{IG}^2) - P_G^2}}{I_{RG}^2 + I_{IG}^2} \quad (8)$$

These nonlinear equations were linearized via a first-order Taylor expansion for Newton-Raphson iterations, leading to a number of equivalent circuit components derived from partial derivatives of equations (7) and (8). Note that if the argument under the square root in either of these is negative, a non-physical solution for voltage arises (e.g., a complex value for real voltage). To prevent this from occurring, damped Newton-Raphson iterations were applied in [2] to reduce the step size if an iteration yielded a non-physical result. The large number of iterations reported in [2] is a direct result of damping, since very small steps were taken to avoid non-physical solutions.

There is an alternate approach to formulating a generator model, however, whereby equations do not contain square roots. From the definition of apparent power  $S = VI^*$ :

$$P_G + jQ_G = (V_{RG} + jV_{IG})(I_{RG} - jI_{IG}) \quad (9)$$

We can solve equations (5) and (9) simultaneously to obtain:

$$I_{RG} = \frac{P_G V_{RG} + Q_G V_{IG}}{V_{RG}^2 + V_{IG}^2} \quad (10)$$

$$I_{IG} = \frac{P_G V_{IG} - Q_G V_{RG}}{V_{RG}^2 + V_{IG}^2} \quad (11)$$

The generator reactive power  $Q_G$  is not known, and so it is added as a variable. An extra equation must be added to keep the number of equations and variables consistent; equation (6) is therefore added as a constraint that ensures the voltage magnitude remains constant and equal to the specified value.

Taylor expansions of equations (10) and (11) are taken to linearize the functions and derive equivalent circuit components. For example, the Taylor expansion of the real generator current about the  $(k + 1)^{th}$  iteration is given by:

$$I_{RG}^{k+1} = \frac{\partial I_{RG}}{\partial Q_G} \Big|_{Q_G^k, V_{RG}^k, V_{IG}^k} (Q_G^{k+1}) + \frac{\partial I_{RG}}{\partial V_{RG}} \Big|_{Q_G^k, V_{RG}^k, V_{IG}^k} (V_{RG}^{k+1}) \quad (12)$$

$$+ \frac{\partial I_{RG}}{\partial V_{IG}} \Big|_{Q_G^k, V_{RG}^k, V_{IG}^k} (V_{IG}^{k+1}) + I_{RG}^k - \frac{\partial I_{RG}}{\partial Q_G} \Big|_{Q_G^k, V_{RG}^k, V_{IG}^k} (Q_G^k)$$

$$- \frac{\partial I_{RG}}{\partial V_{RG}} \Big|_{Q_G^k, V_{RG}^k, V_{IG}^k} (V_{RG}^k) - \frac{\partial I_{RG}}{\partial V_{IG}} \Big|_{Q_G^k, V_{RG}^k, V_{IG}^k} (V_{IG}^k)$$

The second term represents a conductance, because the real current is proportional to the real voltage; the third term represents a voltage-controlled current source, because the real current is proportional to the imaginary voltage. The remaining terms (except for the first) are all dependent on known values from the previous iteration, so they can be lumped together and represented as an independent current source. Figure 2 shows the equivalent circuit with symmetric elements for the real and imaginary generator current. Note that none of the terms contains a square root, which eliminates the need for damping. The implications of this are discussed in the Results section.

The first term in equation (12) is not a true circuit element, as it represents a value of current controlled by reactive power. The equation for this term is appended to our matrix of circuit equations, such that the system in (4) becomes:

$$\begin{bmatrix} 1 - \alpha F^T & RF & 0 \\ -GF^T & 1 + \beta F & \tau \\ \gamma & 0 & 0 \end{bmatrix} \begin{bmatrix} v_t \\ i_l \\ Q_g \end{bmatrix} = \begin{bmatrix} V_t \\ I_l \\ 0 \end{bmatrix} \quad (13)$$

$\tau$  represents the partial derivatives of the generator current (real and imaginary) with respect to  $Q_g$ , and  $\gamma$  represents the linearized constraints derived from (6) to keep the voltage magnitude of a given generator at its prescribed value.

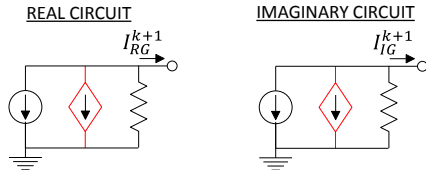


Figure 2 – Generator equivalent circuit model using current sources; the red controlled sources indicate coupling between the real and imaginary sub-circuits.

#### IV. GENERALIZED MODELING: SOLAR ARRAY EXAMPLE

All electrical devices can be characterized by a relationship between current and voltage. In the previous section we derived a nonlinear expression for generator current in terms of voltage based on fixed power and voltage constraints. This approach can be extended to model any nonlinear relationship that describes an element of the power system, allowing for novel models that are not compatible with traditional power flow. As an example, we next derive a model of a solar array to illustrate how generalized modeling in terms of current and voltage can be used to create physical buses that are not capable of being described as constant-PV or constant-PQ.

#### A. Description of Solar System

Figure 3 shows a block diagram of a grid-connected solar system. A DC-to-AC inverter applies a maximum power point tracking (MPPT) control strategy to force the solar array to operate at its maximum power point ( $P_{MPP}$ ), with an output DC voltage of  $V_{MPP}$  and output DC current of  $I_{MPP}$ . The AC output of the inverter is filtered by an RLC circuit and an isolation transformer transfers the generated power ( $P_g$ ) to the grid. We assume  $Q = 0$  since solar systems are commonly designed to operate at unity power factor and that the real power output of the inverter is equal to the solar output ( $P_{MPP}$ ). Figure 3 is similar to the model in [7], but we solve the entire system together and do not treat the bus as fixed-PV or fixed-PQ.

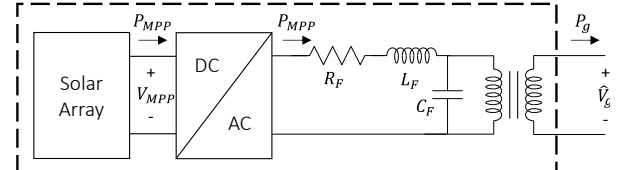


Figure 3 – Block diagram of grid-connected solar system.

#### B. Equivalent Circuit Representation

An equivalent circuit of the system diagram in Figure 3 is shown in Figure 4. The solar array is replaced by a single diode model, where  $I_{PH}$  is the photovoltaic current generated by solar irradiance,  $R_{SH}$  is a parasitic shunt resistance, and  $R_S$  is the series resistance of the array. The inverter loads the array with impedance  $Z_{MPP}$  to force the array to operate at its maximum power point, which occurs when

$$\frac{\partial (I_{MPP} V_{MPP})}{\partial V_{MPP}} = I_{MPP} + V_{MPP} \frac{\partial I_{MPP}}{\partial V_{MPP}} = 0 \quad (14)$$

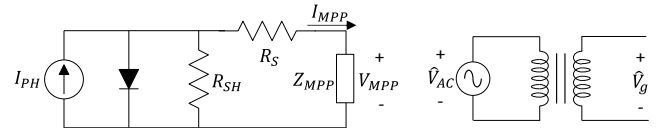


Figure 4 – Equivalent circuit model of solar system.

The AC side represents the output of the inverter.  $\hat{V}_{AC}$  is the voltage that appears at the input to the transformer, and is equal to the output voltage of the inverter minus any voltage drop across the filter elements. The output voltage of the transformer  $\hat{V}_g$  is applied directly to the grid. The real output power  $P_g$  is equal to the generated solar power  $P_{MPP}$  minus any real power losses in the filter and transformer.

#### C. Linearized Split Circuit Model

To solve the circuit in Figure 4 we must linearize it following the same procedures outlined in Section III. The current through the diode ( $I_D$ ) is given by:

$$I_D = I_0 (e^{V_D/a} - 1) \quad (15)$$

where  $I_0$  is the reverse saturation current,  $V_D$  is the diode voltage, and  $a$  is a non-ideality factor. This equation is linearized by taking a first-order Taylor expansion to yield:

$$I_D^{k+1} = I_D^k + \frac{\partial I_D}{\partial V_D} |_{V_D^k} V_D^{k+1} - \frac{\partial I_D}{\partial V_D} |_{V_D^k} V_D^k \quad (16)$$

The first and third terms depend only on values from the previous iteration and can therefore be represented as an independent current source. The second term gives a component of the diode current that is proportional to the diode voltage, and therefore represents a conductance. The parallel combination of these elements replaces the diode in the linearized circuit of Figure 5.

The load the inverter presents to the solar array forces maximum power operation when equation (14) holds. By evaluating the equation at the maximum power point we see the current  $I_{MPP}$  flowing through the load is:

$$I_{MPP} = V_{MPP} \frac{(I_0 R_{SH} \chi - a)}{a(R_{SH} + R_S) + I_0 R_S R_{SH} \chi} \quad (17)$$

where  $\chi = \exp([V_{MPP} + I_{MPP} R_S]/a)$ . By taking a Taylor expansion of equation (17) we again obtain two equivalent circuit elements, an independent current source ( $I_L^k$ ) and a conductance ( $G_L^k$ ). These are shown at the output of the DC circuit in Figure 5. The maximum power point is updated on every iteration until convergence.

The AC side of the circuit must be split into real and imaginary parts. We have assumed the reactive power is zero and that the real output power of the inverter is  $P_{MPP}$ . Using the relationship expressed in equation (5) we can solve for the real and imaginary voltage components of  $\hat{V}_{AC}$  to obtain:

$$V_R = \frac{I_{MPP} V_{MPP}}{I_R^2 + I_I^2} - R_F I_R \quad (18)$$

$$V_I = \frac{I_{MPP} V_{MPP}}{I_R^2 + I_I^2} - R_F I_I \quad (19)$$

Note that we have lumped the voltage drop across the filter resistance into the source values. By taking Taylor expansions of (18) and (19) we obtain the equivalent circuit components shown in Figure 5. The real circuit contains an independent voltage source, two current-controlled voltage sources (one dependent on  $I_I$  and the other on  $I_{MPP}$ ), and one voltage-controlled voltage source (dependent on  $V_{MPP}$ ). Similar elements are shown for the imaginary circuit. The procedure for splitting a transformer is given in [2].

## V. RESULTS AND DISCUSSION

The proposed method was implemented in MATLAB. The program reads in power flow case files in the standard IEEE CDF format and represents each bus and line with circuit element models. The TLA equations are formulated and solved via Newton-Raphson method.

### A. Iteration Count

For robust convergence from arbitrary initial guesses, the voltage source-based generator model in [2] requires damping that leads to excessive iteration counts. The generator model in Section III, however, does not require damping to avoid the non-physical solutions, thereby converging in significantly

fewer iterations. Table I shows that only 5-7 iterations are required to converge to a solution independent of system size for test systems ranging from a few buses to several thousand buses. An arbitrary initial guess was used; a good initial guess would further reduce the iteration count.

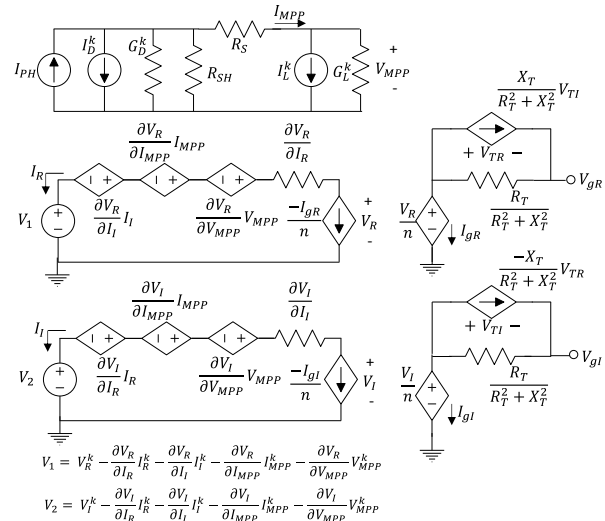


Figure 5 – Linearized circuit model of the solar system.

Beyond the elimination of damping for arbitrary initial guess, the proposed current source generator model may provide faster convergence because it expresses the generator in terms of the more “natural” variable. A typical solution in a power system is one where the load voltages are high ( $\approx 1$  p.u.) and the currents are correspondingly low to satisfy  $S = VI^*$ , where  $S$  is given. The generators, of course, supply the current to the system. For these high voltage/low current solutions, the generator is therefore better suited as a link element in the TLA formulation. Being able to model a bus in multiple ways to choose the easiest variable to solve for further illustrates the flexibility of this method; in traditional power flow, there is only one way to model a generator or a load.

Table I – Iteration counts for test systems using voltage source-based (VS) generator models with damping and current source-based (CS) generator models without damping.

#Buses	14	30	57	118	300	2383	3120
VS Model [2]	29	30	30	98	265	-	-
CS Model	5	5	5	5	6	7	7

### B. Convergence and Robustness

Traditional power flow is known to be sensitive to the initial guess [2],[8], which can be represented as a point on a complex plane with real voltage as the x-axis and imaginary voltage as the y-axis. The result for a sweep of 10000 initial guesses for load voltage in the IEEE 30-bus case using our method is shown in Figure 6, where green points represent convergence to the correct solution and red points represent convergence to a spurious solution. Roughly 96% of initial guesses, even poor ones, ultimately yield the correct solution.

To further improve convergence, we implemented a power stepping algorithm borrowed from circuit simulation [9]. A common method to find the DC solution to a nonlinear circuit

is to scale down the supply voltage to a small value, where all node voltages are nearly zero and an initial guess of zero works well. The supply is then incrementally stepped up to its original value, using the previous condition's solution as the initial guess for each iteration. This is akin to simulating the "turning on of the circuit," and can be applied to the "turning on of the grid." All real power is first scaled down by 1000x. The solution to this system is used as the initial guess for the next iteration where the loads are increased, and this is repeated until all loads are returned to their initial values. The inset of Figure 6 illustrates that any initial guess can work when this method is applied.

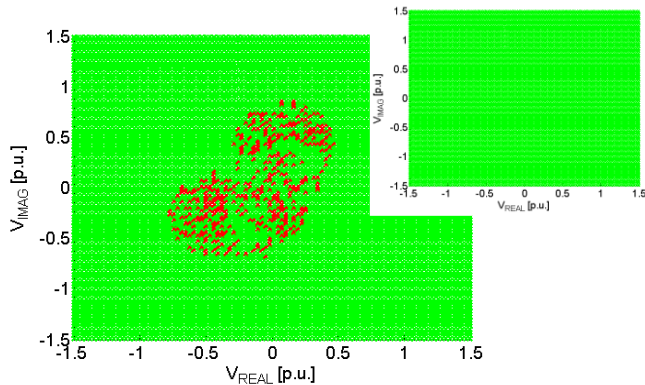


**Figure 6 – Roughly 96% of initial guesses for load voltage yield the correct solution (green points) in the 30-bus system; (inset) any initial guess works when power stepping is applied.**

Importantly, power stepping is only applicable to our formulation. In traditional power flow, the Jacobian is constructed from derivatives with respect to voltage magnitude and phase; if power is scaled, nothing in the Jacobian changes because the derivatives of constant power terms are zero, and so convergence is not improved. The results demonstrated here are another benefit of working with physical models and the true state variables of the system.

### C. Integration of Solar Model

To demonstrate the use of the generalized solar bus model, we removed a generator from the IEEE 14-bus system and replaced it with the equivalent model in Figure 3. The solar array was designed to output 40 MW, the same real power that was delivered by the generator it replaced. The AC voltages and currents of the model were scaled to their per unit values to be compatible with the rest of the system, but the DC circuit was solved with standard units.

The generalized circuit-based modeling allows the DC and AC circuits to be solved together with the same algorithm and without having to fit the model to a PQ- or PV-bus type, in contrast to other approaches [7]. As the DC circuit converges to the maximum power point, the AC side transfers that power output to the rest of the grid. Convergence is obtained in seven iterations with no damping and an absolute tolerance of  $1e-4$  p.u. The solar array and slack bus are the only sources of real power in the system, and we observe the output power of the latter decreases with increasing solar power injected into the network (Figure 7).

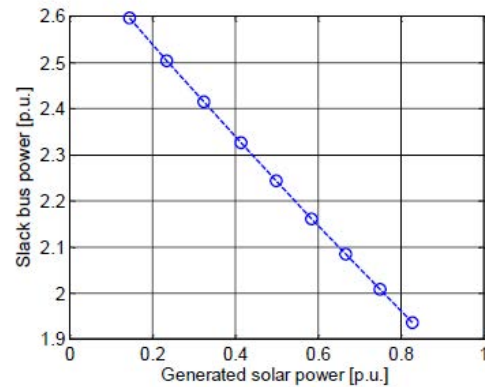


**Figure 7 – Slack bus power output decreases as the solar array supplies more power to the system.**

## VI. CONCLUSION

We have presented an approach for single phase power flow based on equivalent circuits with current and voltage variables. By expressing the equations in terms of the true state variables, we show that nonlinear relationships between current and voltage can be efficiently handled with excellent convergence behavior. A new current source-based generator model was introduced that significantly reduces the iteration count compared to a previous implementation. The approach facilitates generalized modeling in terms of current and voltage that enables simulation with a wide range of complex nonlinear models.

## ACKNOWLEDGMENT

This research is funded in part by the CMU-SYSU Collaborative Innovation Research Center and the SYSU-CMU International Joint Research Institute.

## REFERENCES

- [1] W. F. Tinney, C. E. Hart, "Power Flow Solution by Newton's Method," *IEEE Transactions on Power Apparatus and Systems*, volume PAS-86, issue 11, Nov. 1967.
- [2] D. M. Bromberg, M. Jereminov, X. Li, G. Hug, L. Pileggi, "An Equivalent Circuit Formulation of the Power Flow Problem with Current and Voltage State Variables," *2015 IEEE PowerTech Eindhoven (POWERTECH)*, 2015.
- [3] L.W. Nagel and D.O. Pederson, "SPICE (Simulation Program with Integrated Circuit Emphasis), EECS Department, University of California, Berkeley UCB/ERL M382, April 1973.
- [4] R. D. Zimmerman, C. E. Murillo-Sánchez, and R. J. Thomas, "MATPOWER: Steady-State Operations, Planning and Analysis Tools for Power Systems Research and Education," *IEEE Transactions on Power Systems*, vol. 26, no. 1, pp. 12-19, Feb. 2011.
- [5] L. Pillage, R. Rohrer, C. Visweswariah, *Electronic Circuit & System Simulation Methods*, McGraw-Hill, Inc., New York, NY, USA, 1995.
- [6] P. M. Russo and R. A. Rohrer, "The Tree-link Analysis Approach to Network Analysis," *IEEE Transactions on Circuit Theory*, vol. CT-18(3), pp. 400-403, May 1971.
- [7] Y.-B. Wang, C.-S. Wu, L. Hua, H.-H. Xu, "Steady-State Model and Power Flow Analysis of Grid-Connected Photovoltaic Power System," *IEEE International Conference on Industrial Technology*, 2008.
- [8] A. Trias, "The Holomorphic Embedding Load Flow Method," *IEEE PES General Meeting*, July 2012.
- [9] F. H. Branin Jr., H. H. Wang, "A fast reliable iteration method for dc analysis of nonlinear networks," *Proc. IEEE*, vol. 55, pp. 1819-1826 1967.